DE GRUYTER OPEN
www.czasopisma.pan.pl PAN POLSKA AKADEMIA NAUK www.journals.pan.pl
Chemical and Process Engineering 2016, 37 (2), 199-213
DOI: 10.1515/cpe-2016-0017

SIMULATION OF HEAT TRANSFER IN COMBUSTION CHAMBER WATERWALL TUBES OF SUPERCRITICAL STEAM BOILERS

Sławomir Grądziel*, Karol Majewski

Cracow University of Technology, Institute of Thermal Power Engineering, al. Jana Pawła II 37, 31-864 Kraków, Poland

The paper presents the results of numerical computations performed for the furnace chamber waterwalls of a supercritical boiler with a steam output of 2400×10^3 kg/h. A model of distributed parameters is proposed for the waterwall operation simulation. It is based on the solution of equations describing the mass, momentum and energy conservation laws. The aim of the calculations was to determine the distribution of enthalpy, mass flow and fluid pressure in tubes. The balance equations can be brought to a form where on the left-hand side space derivatives, and on the right-hand side – time derivatives are obtained. The time derivatives on the right-hand side were replaced with backward difference quotients. This system of ordinary differential equations was solved using the Runge-Kutta method. The calculation also takes account of the variable thermal load of the chamber along its height. This thermal load distribution is known from the calculations of the heat exchange in the combustion chamber. The calculations were carried out with the zone method.

Keywords: waterwall tubes, supercritical steam boiler, mathematical model, energy balance, thermal load

1. INTRODUCTION

Nowadays an increase in the price of fuel and regulations aimed at natural environment protection are observed. Companies generating electrical power and suppliers of technologies for power plants are forced to improve the efficiency of using the fossil fuel chemical energy. This is developed in a number of ways. One of them is constructing high-efficiency power units with the main component being a once-through steam boiler with supercritical or ultrasupercritical steam parameters (Taler, 2011). The capacity of power units can be increased by using high parameters of steam, high-capacity turbines, lower pressure in the condenser and a double or triple interstage steam superheating. Previous solutions used a fresh steam temperature of 560 - 610°C and a pressure of 26 - 30 MPa. At present over two hundred units with supercritical steam parameters operate globally. The installed power in the largest one is 1300 MW and fresh steam parameters are as follows: t = 600 °C, p = 35 MPa.

With the new supercritical steam power blocks a number of new problems and issues related to the operation of these blocks arise (Błaszczuk at al., 2014; Kotowicz and Michalski, 2014; Pronobis and Litka, 2012).

Problems encountered when modelling transient processes of heat and flow in heated surfaces of power boilers show that these processes are complex and highly nonlinear. The complexity is caused by the high values of temperature and pressure, the cross-parallel or cross-counter-flow of fluids and large

*Corresponding author, e-mail: gradziel@mech.pk.edu.pl

heat transfer surfaces (ranging from several hundred to several thousand square metres). Moreover, the increasing fouling of these surfaces on the combustion gases side causes changes in heat transfer conditions. In many studies the influence of deposit formations on heat transfer process are shown. Taler et al. (2011) presented numerical modelling of boiler superheater that takes into account deposit formation on heating surfaces. Modliński (2014) presented CFD calculation for similar problems focused on boiler combustion chamber.

Various methodologies and ways of calculating the thermal and flow parameters in a forced circulation boiler have been presented by many authors (Adam and Marchetti, 1999; Kim and Choi, 2005; Stosic and Stevanovic, 2003; Tucakovic and al., 2007). The calculations took into account all principal thermal and flow parameters along the entire length of the operating tubes of the evaporator. Tucakovic et al., (2007) focused in their work on the differences between the rifled and smooth tubes used in boiler evaporators. In design calculations it is assumed that the evaporator may operate with natural water circulation, i.e. no circulation pump needs to be incorporated into the evaporator system. However, the presented model employs simplified energy balance equations only.

Steam boilers with supercritical parameters are designed as Benson type once-through boilers. They can be constructed as single-pass or double-pass (tower) boilers. The furnace chamber walls can be made with a vertical or spiral arrangement of the pipes. A spiral arrangement of the pipes on the furnace chamber walls makes each pipe pass through four walls, which significantly reduces the differences in the pipe lengths and the quantity of absorbed heat. This arrangement ensures adjusting the medium temperatures at the wall outlets even with great differences in the quantity of heat absorbed by each wall.

The power unit featuring supercritical steam parameters, with a capacity of 858 MW was installed at the Bełchatów Power Plant in Poland. The main parameters of the boiler are as follows: steam output capacity 2400×10^3 kg/h, live steam pressure p = 26.6 MPa, live steam temperature 554 °C, reheated steam pressure 5.4 MPa, reheated steam temperature 582°C.

The paper presents the results of numerical computations performed for the furnace chamber waterwalls of a supercritical boiler with a steam capacity of 2400×10^3 kg/h. The model of distributed parameters is proposed for the evaporator operation simulation. The model is based on the solution of equations describing the mass, momentum and energy conservation laws. The aim of the calculations was to determine the distribution of enthalpy, mass flow and fluid pressure in tubes.

The proposed mathematical model was also verified experimentally. The verification was based on the comparison of calculated and measured values of temperature at the boiler tube outlet.

2. MATHEMATICAL MODEL

This chapter presents a proposal for the waterwall distributed parameter model based on the solution of equations describing the mass, momentum and energy conservation laws. General principles that describe the equations for fluid flows are presented in (Bishop et al., 1965; Slattery, 1999; Welty et al., 2008).

Dependences shown below result from an analysis of the characteristics of a stream flowing into and out of an infinitely small control volume (Fig. 1). The equations are written for the flow in the direction of axis z.

The heat conduction equation for the wall separating the fluid was also derived. The wall was divided into two control volumes, which made it possible to calculate the temperature on its both sides: on the combustion gas side and on the heated fluid side.

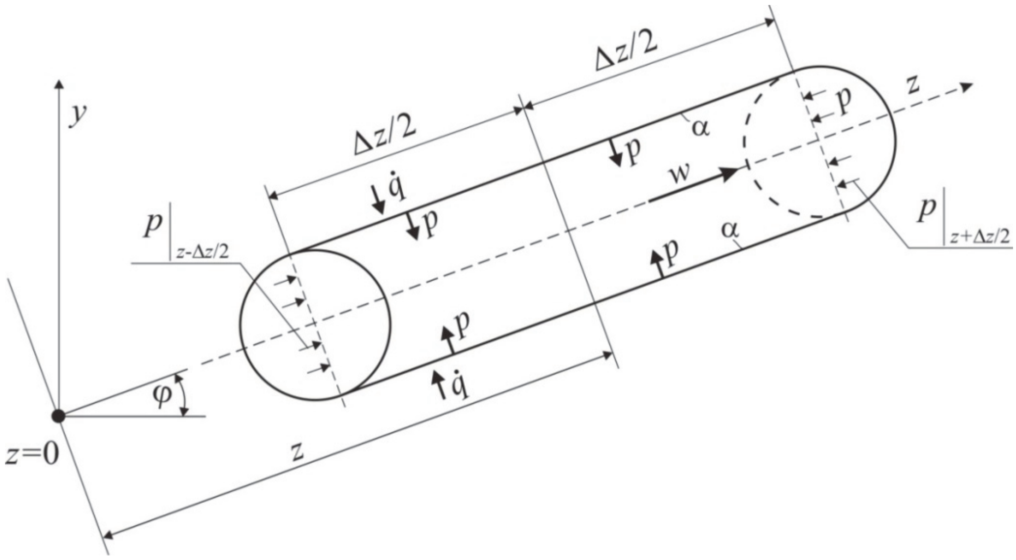

Fig. 1. Analysed control volume (CV) with length Δz; φ – CV horizontal deviation angle

2.1. Mass conservation law

The following is derived from the mass balance equation for the control volume with finite volume ΔV presented in Fig. 1:

$$\frac{\partial(\Delta V \rho)}{\partial \tau} = (A\rho w)\Big|_{z-\Delta z/2} - (A\rho w)\Big|_{z+\Delta z/2} \tag{1}$$

where:

$$\Delta V = A \cdot \Delta z \tag{2}$$

It is also assumed that Δz is sufficiently small and the average density in the entire volume ΔV is equal to the fluid density in the centre of gravity *Z*.

Considering dependence (1) in Eq. (2) and dividing both sides of the equation by Δz, the following is obtained:

$$\frac{\partial(A\rho)}{\partial \tau} = -\frac{(A\rho w)\big|_{z+\Delta z/2} - (A\rho w)\big|_{z-\Delta z/2}}{\Delta z} \tag{3}$$

If $\Delta z \to 0$, then

$$\frac{\partial(A\rho)}{\partial \tau} = -\frac{\partial(A\rho w)}{\partial z} \tag{4}$$

Simple transformations result in:

$$\frac{\partial \rho}{\partial \tau} = -\frac{\partial}{\partial z}(\rho w) \tag{5}$$

or

$$\frac{\partial \rho}{\partial \tau} = -\frac{1}{A}\frac{\partial \dot{m}}{\partial z} \tag{6}$$

where $\dot{m} = A\rho w$ denotes the mass flow of a fluid flowing through a duct.

2.2. Momentum conservation law

The momentum balance equation for the volume control, apart from the momentum flux flowing in and out and beside the rate of changes in accumulated momentum, has to take account all forces affecting the control volume. These forces can be divided into surface forces and body forces. The former include forces exerted by pressure, which are opposite to the normal to the inlet and outlet surface area, the force exerted by the wall surface and the friction force occurring on the inside surface of a duct. The force exerted by the wall on the fluid contained in the control volume is equal to the product of the wall surface area $A\big|_z = U\big|_z \cdot \Delta z$ (where U denotes circumference) and pressure p. In our analysis, the component of this force in the direction of coordinate z is zero $\left(A\big|_{z-\Delta z/2} = A\big|_{z+\Delta z/2}\right)$.

The friction force acts opposite to the direction of the fluid flow and equals the product of the wall surface area $U\Delta z$ and tangential stress σ_τ on the wall surface. The momentum conservation equation can thus be written as:

$$\frac{\partial}{\partial \tau}(A\Delta z \rho w) = (\dot{m}w)\bigg|_{z-\Delta z/2} - (\dot{m}w)\bigg|_{z+\Delta z/2} + A\left(p\bigg|_{z-\Delta z/2} - p\bigg|_{z+\Delta z/2}\right) - \sigma_\tau U\Delta z - \Delta V \rho g \sin\varphi \tag{7}$$

Assuming that $\Delta z \to 0$, Eq. (7) takes the form:

$$\frac{\partial(A\rho w)}{\partial \tau} = -\frac{\partial(\dot{m}w)}{\partial z} - \frac{\partial(Ap)}{\partial z} - \sigma_\tau U - A\rho g \sin\varphi \tag{8}$$

Using the dependence resulting from the condition of equilibrium of forces:

$$\sigma_\tau U\Delta z = A\Delta p_\tau \quad \Rightarrow \quad \sigma_\tau U = A\frac{\partial p_\tau}{\partial z} \tag{9}$$

and the dependence:

$$w = \frac{\dot{m}}{A\rho} \tag{10}$$

Eq. (8) takes the following form:

$$\frac{\partial \dot{m}}{\partial \tau} = -\frac{1}{A}\frac{\partial}{\partial z}\left(\frac{\dot{m}^2}{\rho}\right) - A\left(\frac{\partial p}{\partial z} + \frac{\partial p_\tau}{\partial z} + \rho g \sin\varphi\right) \tag{11}$$

The friction-related pressure drop in Eq. (11) is defined based on the Darcy-Weisbach equation:

$$\frac{\partial p_\tau}{\partial z} = \frac{\sigma_\tau U}{A} = \frac{\zeta\, \dot{m}^2}{2d_{in}\rho A^2} = \frac{\zeta}{d_{in}}\frac{\dot{m}|\dot{m}|}{2\rho A^2} \tag{12}$$

2.3. Energy conservation law

The energy conservation equation for the control volume presented in Fig. 1 is as follows:

$$\frac{\partial}{\partial \tau}(\Delta V \rho e) = A\left(\rho w e\bigg|_{z-\Delta z/2} - \rho w e\bigg|_{z+\Delta z/2}\right) + \dot{q}U\Delta z + A\left[-k\frac{\partial t}{\partial z}\bigg|_{z-\Delta z/2} - \left(-k\frac{\partial t}{\partial z}\right)\bigg|_{z+\Delta z/2}\right] + $$

$$+ A\left(pw\bigg|_{z-\Delta z/2} - pw\bigg|_{z+\Delta z/2}\right) \tag{13}$$

Considering that the total internal energy is:

$$\rho e = \rho u + \rho \frac{w^2}{2} + \rho g\, z \sin\varphi \tag{14}$$

Eq. (13) for $\Delta z \to 0$ is now given by:

$$\mathrm{d}V \frac{\partial}{\partial \tau}\left(\rho u + \frac{1}{2}\rho w^2\right) = -\mathrm{d}V \frac{\partial}{\partial z}\left(\rho u w + \frac{1}{2}\rho w^2 w\right) - \rho w g \sin\varphi + \dot{q} U \mathrm{d}z + \mathrm{d}V \frac{\partial}{\partial z}\left(k \frac{\partial t}{\partial z}\right) - \mathrm{d}V \frac{\partial}{\partial z}(p w) \tag{15}$$

After simple transformations, Eq. (15) can also be presented as:

$$\frac{\partial h}{\partial \tau} = \frac{\dot{m}}{A\rho}\left(\frac{1}{\rho}\frac{\partial p}{\partial z} - \frac{\partial h}{\partial z} + \frac{1}{\rho}\frac{\partial p_\tau}{\partial z}\right) + \frac{\dot{q}U}{A\rho} + \frac{1}{\rho}\frac{\partial}{\partial z}\left(k\frac{\partial t}{\partial z}\right) + \frac{1}{\rho}\frac{\partial p}{\partial \tau} \tag{16}$$

Considering external sources:

$$\dot{q} = \alpha(\theta - t) \tag{17}$$

and replacing the time derivative of pressure (bearing in mind the dependence of pressure on density and enthalpy):

$$\frac{\partial p}{\partial \tau} = \frac{\partial p}{\partial \rho}\frac{\partial \rho}{\partial \tau} + \frac{\partial p}{\partial h}\frac{\partial h}{\partial \tau} = -\frac{1}{A}\frac{\partial p}{\partial \rho}\frac{\partial \dot{m}}{\partial z} + \frac{\partial p}{\partial h}\frac{\partial h}{\partial \tau} \tag{18}$$

and ignoring heat conductivity in the fluid, the final form of the energy balance equation is obtained:

$$\frac{\partial h}{\partial \tau} = \left(1 - \frac{1}{\rho}\frac{\partial p}{\partial h}\right)^{-1}\left[\frac{\dot{m}}{A\rho}\left(\frac{1}{\rho}\frac{\partial p}{\partial z} - \frac{\partial h}{\partial z} + \frac{1}{\rho}\frac{\partial p_\tau}{\partial z}\right) + \frac{4\alpha(\theta - t)}{d_{in}\rho} - \frac{1}{A\rho}\frac{\partial p}{\partial \rho}\frac{\partial \dot{m}}{\partial z}\right] \tag{19}$$

2.4. Solving balance equations for waterwall tubes

To solve balance equations (6), (11) and (19) a method will be proposed below. Dependencies will be derived that allow a determination of distributions of the mass flow from the stream continuity equation, pressure – from the equation of motion, and enthalpy – from the energy balance equation. Appropriately written equations will make up a mathematical model suitable for analysing thermal and flow phenomena occurring in boiler waterwalls.

After some simplifications and transformations, the balance Eqs. (6), (11) and (19) can be brought to a form where on the left-hand side space derivatives, and on the right-hand side – time derivatives are obtained (Zima et al., 2010; Zima and Grądziel, 2013):

- mass conservation equation:

$$\frac{\partial \dot{m}}{\partial z} = -A\frac{\partial \rho}{\partial \tau} \tag{20}$$

- momentum balance equation:

$$\frac{\partial}{\partial z}\left(\frac{\dot{m}^2}{A^2\rho} + p\right) = -\frac{1}{A}\frac{\partial \dot{m}}{\partial \tau} - \frac{\partial p_\tau}{\partial z} - \rho g \sin\varphi \tag{21}$$

- energy balance equation:

$$\frac{\partial h}{\partial z} = \frac{\rho A}{\dot{m}}\left(-\frac{\partial h}{\partial \tau} + \frac{4\alpha(\theta - t)}{d_{in}\rho}\right) \tag{22}$$

The time derivatives on the right-hand side were replaced with backward difference quotients. This system of ordinary differential equations is solved using the Runge-Kutta method.

After the described changes are introduced, the energy balance equation has the following form:

$$\frac{\mathrm{d}h_j^\tau}{\mathrm{d}z} = \frac{\rho_j^{\tau-\Delta\tau} A}{\dot{m}_j^{\tau-\Delta\tau}} \left(-\frac{h_j^\tau - h_j^{\tau-\Delta\tau}}{\Delta\tau} + \frac{4\alpha_j^{\tau-\Delta\tau}\left(\theta_j^{\tau-\Delta\tau} - t_j^{\tau-\Delta\tau}\right)}{d_{in}\rho_j^{\tau-\Delta\tau}} \right) \tag{23}$$

The fluid density is found as a function of enthalpy and pressure:

$$\rho_j^\tau = f\left(h_j, p_j^{\tau-\Delta\tau}\right) \tag{24}$$

Solving the mass and momentum conservation equations, the following is obtained, respectively:

$$\frac{\mathrm{d}\dot{m}_j^\tau}{\mathrm{d}z} = -A\frac{\rho_j^\tau - \rho_j^{\tau-\Delta\tau}}{\Delta\tau} \tag{25}$$

$$\frac{\mathrm{d}}{\mathrm{d}z}\left(\frac{\left(\dot{m}^2\right)_j^\tau}{A^2\rho_j^\tau} + p_j^\tau \right) = -\frac{1}{A}\frac{\left(\dot{m}^2\right)_j^\tau - \left(\dot{m}^2\right)_j^{\tau-\Delta\tau}}{\Delta\tau} - \frac{dp_\tau}{dz} - \rho_j g \sin\varphi \tag{26}$$

The fluid temperature curve is found as a function of enthalpy and pressure:

$$t_j^\tau = f\left(h_j^\tau, p_j^\tau\right) \tag{27}$$

Subscript "j" in Eqs. (23-27) denotes the number of analysed cross-sections and varies in the range of $j = 2\ldots M$. All thermophysical properties of the fluid and of the wall, as well as the heat transfer coefficient, are determined systematically.

Moreover, in the case of the presented method the Courant condition should be satisfied (Gerald and Wheatley, 1994):

$$\Delta\tau \le \frac{\Delta z}{w} \tag{28}$$

This is a stability condition imposed on the time step to ensure transposition of the numerical solution with velocity $\Delta z/\Delta\tau$ higher than physical velocity w.

2.5. Energy balance equation for the wall

The time- and space-dependent distribution of the tube wall temperature will be found from the transient heat conduction equation:

$$c_w(\theta)\rho_w(\theta)\frac{\partial\theta}{\partial\tau} = \frac{1}{r}\frac{\partial}{\partial r}\left[r k_w(\theta)\frac{\partial\theta}{\partial r} \right] \tag{29}$$

Uniform heating of the tube with a heat flux with equivalent density $\dot{q}_e$ flowing onto the tube pitch (Fig. 2) is assumed.

Equation (29) will be solved taking account of the wall mean temperature θ:

$$c_w\rho_w\frac{\left(r_o^2 - r_{in}^2\right)}{2}\frac{\partial\theta}{\partial\tau} = \left[r k_w(\theta)\frac{\partial\theta}{\partial r} \right]\Bigg|_{r=r_o} - \left[r k_w(\theta)\frac{\partial\theta}{\partial r} \right]\Bigg|_{r=r_{in}} \tag{30}$$

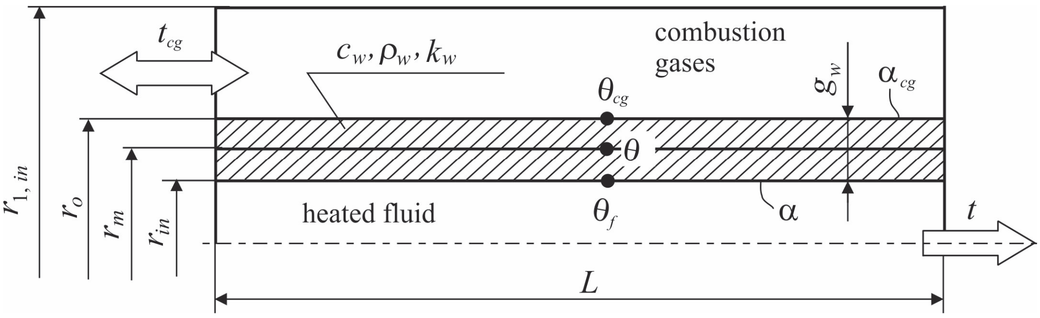

Fig. 2. Division of the wall separating working fluids into two control volumes

under the following boundary conditions:

$$k_w \left.\frac{\partial \theta}{\partial r}\right|_{r=r_o} = \dot{q}_e \tag{31}$$

$$k_w \left.\frac{\partial \theta}{\partial r}\right|_{r=r_{in}} = \alpha\left(\theta|_{r=r_{in}} - t\right) = \alpha(\theta - t) \tag{32}$$

Substituting (31) and (32) in (30), a system of ordinary differential equations is obtained:

$$D\frac{\mathrm{d}\theta}{\mathrm{d}\tau} = t - \theta + G\Delta q \tag{33}$$

where: $D = \dfrac{c_w \rho_w \, d_m \, g_w}{\alpha d_{in}}$, $G = \dfrac{1}{\alpha \pi d_{in}}$, $d_m = \dfrac{d_o + d_{in}}{2}$, $\Delta q = \dot{q} \cdot \mathrm{s} = \dot{q}_e \cdot \pi \cdot d_o$.

Factor D is a time constant characterising the tube thermal inertia. Factor G describes resistance of the heat transfer from the tube inner surface to the fluid.

Substituting the time derivative in Eq. (30) with the forward difference quotient, the following is obtained after transformations:

$$\theta_j^{\tau+\Delta\tau} = \left(\frac{D_j^\tau}{D_j^\tau + \Delta\tau}\right)\theta_j^\tau + \left(\frac{\Delta\tau}{\Delta\tau + D_j^\tau}\right)\left(t_j^{\tau+\Delta\tau} + G_j^\tau \Delta q_j^{\tau+\Delta\tau}\right); \quad j = 1,\ldots,M \tag{34}$$

All thermophysical properties of the fluid and of the waterwall tube material are calculated systematically, using functions and sub-programs developed based on literature data (Meyer, 1993; Taler and Duda, 2006; Water & Steam, 1999). The history of the heat transfer coefficient α is also determined systematically.

The distribution of the waterwall thermal load, in the form of the heat flux density $\dot{q}$ [W/m^2], is known from the boiler furnace chamber thermal calculations. The calculations are performed using the CKTI or the zone methods (Grądziel, 2008; Grądziel, 2012; Zima and Grądziel, 2013).

3. SIMULATION OF THERMAL AND FLOW PHENOMENA IN THE SUPERCRITICAL BOILER FURNACE CHAMBER WATERWALLS

This chapter presents the results of numerical computations performed for the furnace chamber waterwalls of a supercritical boiler. The calculations were made by means of the methods proposed in

Section 2 to simulate the thermal and flow processes occurring in steam superheaters. The fluid flow in the supercritical boiler furnace chamber waterwalls is a single-phase flow because above the critical point water changes into the gaseous state, skipping the evaporation process. Bearing this in mind, functions and programs were developed to allow on-line calculations of water and steam thermophysical properties in the range and above the critical point. The computations were carried out with the Fortran code (Fortran PowerStation 4.0, 1995).

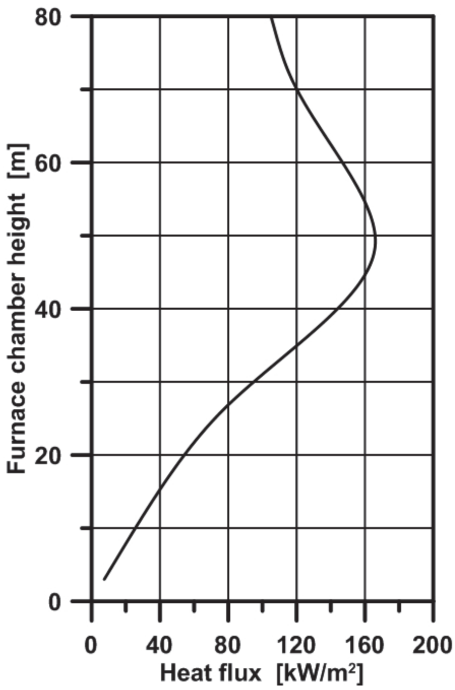

Fig. 3. Distribution of the thermal load of the furnace chamber waterwalls selected for the calculations

The tests were supplemented with calculations taking account of the variable thermal load of the chamber along its height. The thermal load distribution is known from the calculations of the heat transfer in the furnace chamber. The calculations were carried out using the zone method (Grądziel, 2008; Grądziel, 2012). The heat flux density distribution found by means of the zone method, along the furnace chamber height, is shown in Fig. 3.

The proposed method is based on the assumption that the operating fluid flows uniformly through all analysed tubes (in this case – through all tubes of the combustion chamber waterwalls).

The computations concern a lignite-fired boiler. For numerical analysis, the assumed data are those of a boiler operating in one of the Polish power plants (the boiler nominal power output capacity: $N = 858$ MW, live steam pressure: $p = 26.6$ MPa, live steam temperature: $t = 554$ °C).

The boiler furnace chamber was designed as a 23.16 × 23.16 m square. The chamber spiral waterwalls are made of smooth tubes and divided into two parts. In the bottom part, the tubes are arranged at $\varphi = 24.62^o$ and in the upper part – at the angle $\varphi = 28.36^o$. The bottom part is approximately 32 meters high; the tubes are made of 16Mo3 steel ($d_o \times g_w = 33.7 \times 6.3$ mm, $s = 50$ mm). The upper part is located above the pulverised fuel burners. In it, the tubes have a larger diameter ($d_o \times g_w = 38{\times}6.3$ mm, $s = 57$ mm) and they are made of a material which can operate at higher temperatures (13CrMo4-5 steel) (Fig. 4) (Wojciechowski, 2012).

The following data were assumed for the computations (Wojciechowski, 2012):

- total mass flow: $\dot{m}_t = 2400 \times 10^3$ kg/h,
- water pressure at the waterwall inlet: $p_{inlet} = 29.96$ MPa,
- steam pressure at the waterwall outlet: $p_{out} = 28.49$ MPa,

- number of waterwall tubes: $n = 768$,
- length of tubes: $L = 166$ m,
- feed water temperature at the furnace chamber waterwalls inlet: $t = 313.4$ °C,
- steam temperature at the furnace chamber waterwalls outlet: $t = 427.0$ °C,
- waterwall tube material: 16Mo3 and 13CrMo4-5,
- tube outer diameter × tube wall thickness: $d_o \times g_w$=33.7 × 6.1 mm and $d_o \times g_w$=38 × 6.3 mm,
- inclination angle of waterwall tubes : $\varphi = 24.62°$ and $\varphi = 28.36°$,
- tube pitch: $s = 50$ mm and $s = 57$ mm,
- time step: $\Delta\tau = 0.05$ s,
- spatial size of control volume: $\Delta z = 0.5$ m.

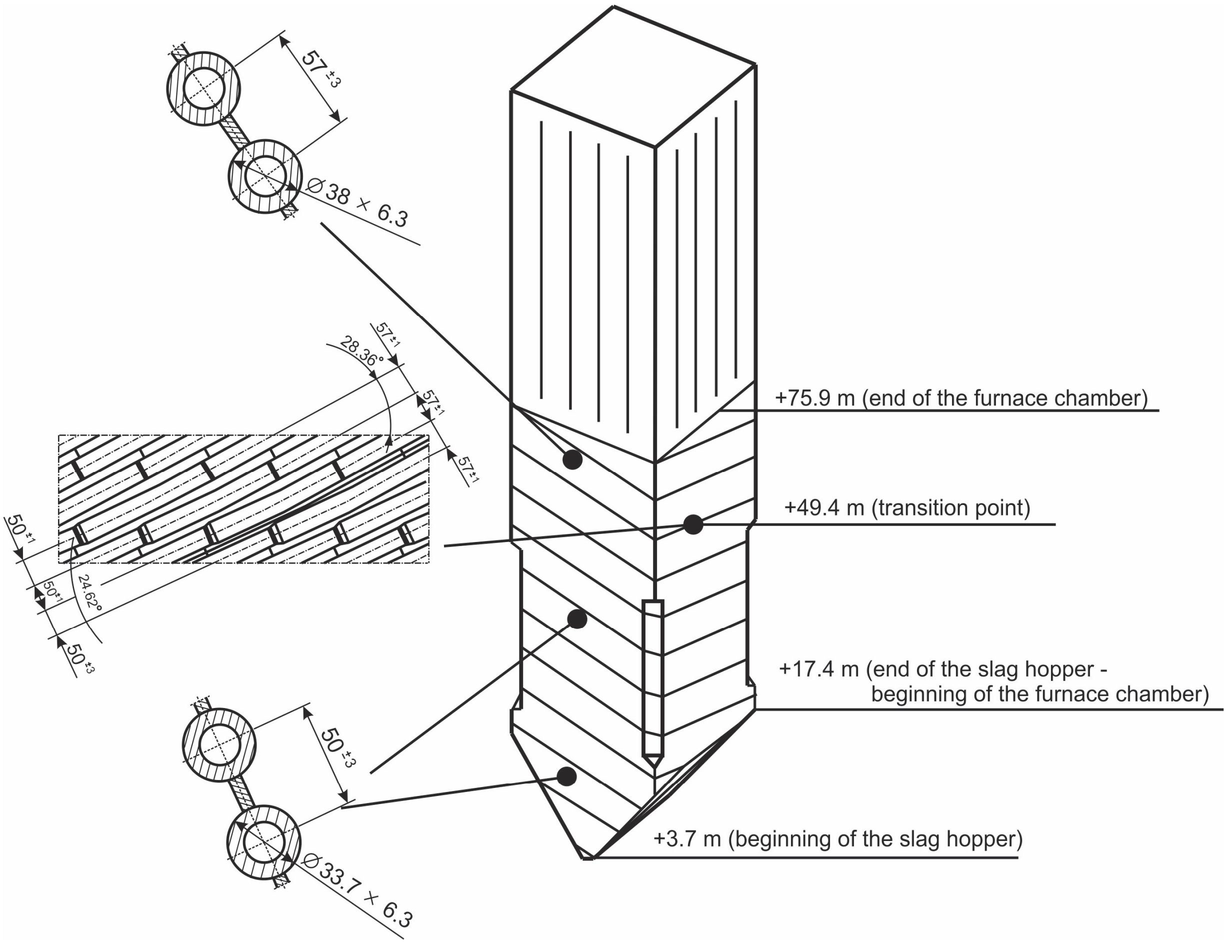

Fig. 4. Diagram of the furnace chamber

In order to find the time- and space-dependent distribution of the working fluid enthalpy it is necessary to know the heat transfer coefficient. Reference literature offers many empirical formulae which allow the calculation of this coefficient values on the inner surface of the waterwall tubes, at pressures higher than critical. In the case of plain (smooth) tubes the equations presented in (Bishop et al., 1965; Jackson, 2002; Kitoh et al., 1999; Tang et al., 2007) can be used.

The heat transfer coefficient was calculated using the Kitoh formula (Kitoh et al., 1999):

$$\mathrm{Nu_b} = 0.015\,\mathrm{Re_b^{0.85}}\,\mathrm{Pr_b^m}, \tag{35}$$

where: $m = 0.69 - \dfrac{81000}{q_{dht}} + f_c q$, $q_{dht} = 200G^{1.2}$, and:

$$f_c = 29\times10^{-8} + \frac{0.11}{q_{dht}} \quad \text{for } 0 \le h_b \le 1500 \text{ kJ/kg,} \tag{36}$$

$$f_c = -8.7\times10^{-8} - \frac{0.65}{q_{dht}} \text{ for } 1500 \le h_b \le 3300 \text{ kJ/kg} \tag{37}$$

$$f_c = -9.7\times10^{-7} + \frac{1.3}{q_{dht}} \text{ for } 3300 \le h_b \le 4000 \text{ kJ/kg.} \tag{38}$$

Dependence (35) was derived for the following ranges:

- fluid bulk temperature: t_b = 20 – 550 °C,
- fluid bulk enthalpy: h_b = 100 – 3300 kJ/kg,
- mass flux: G = 100 – 1750 kg/(m^{2}s),
- thermal load of waterwalls: $\dot{q}$ = 0.0 – 1.8 MW/m^2.

3.1. Numerical analysis

The numerical calculations related to modelling thermal and flow processes occurring in the furnace chamber waterwalls of the boiler under analysis were made for the data presented in Section 3, assuming a variable thermal load along the chamber height (Fig. 3). The results obtained by means of the method described herein are presented taking account the dependence of the fluid thermophysical properties on temperature and pressure, and of the waterwall tube material – on temperature.

The computation results for the selected cross-sections are presented in Figs 5 to 8.

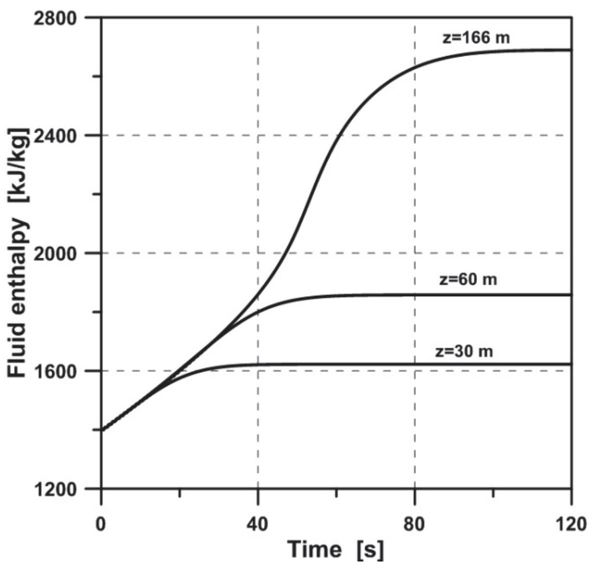

Fig. 5. Fluid enthalpy histories

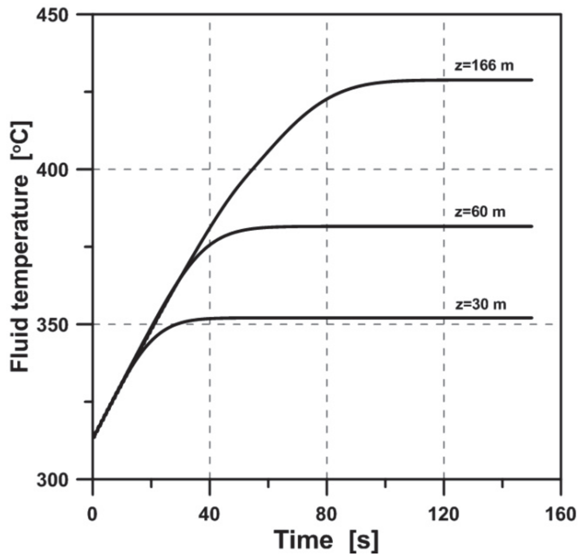

Fig. 6. Fluid temperature histories

An analysis of Fig. 8 indicates that the fluid mass flux reaches values recommended for once-through boilers with the spiral tube arrangement. For lignite, these values should be at the level of 2200 kg/(m^2·s) (Kuznetsov et al., 1973).

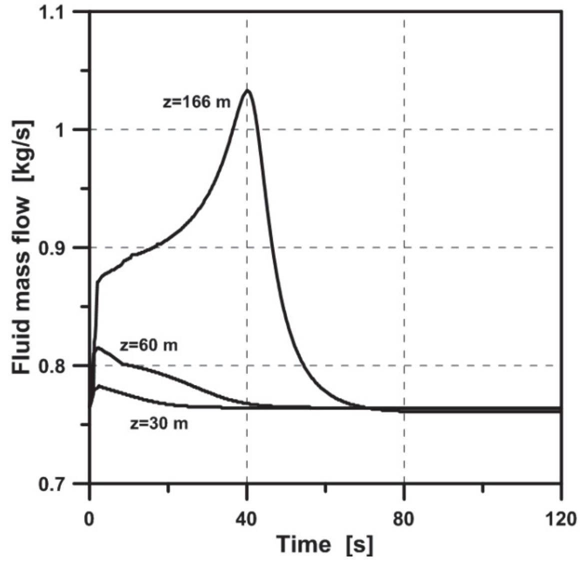

Fig. 7. Fluid mass flow rate histories

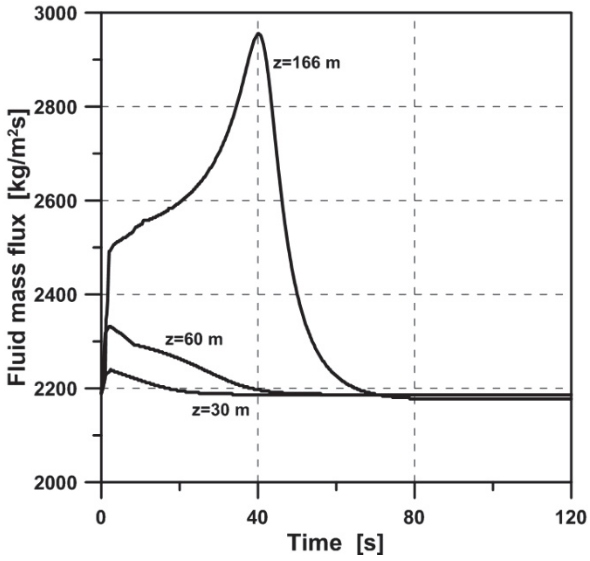

Fig. 8. Histories of the fluid mass flux in selected cross-sections

The curves illustrating the coefficient of the heat transfer from the waterwall tube inner surface to the fluid, calculated using the Kitoh formula (48), are shown in Fig. 9. As an example of thermophysical properties computed in the on-line mode, the obtained histories of the fluid density are shown in Fig. 10.

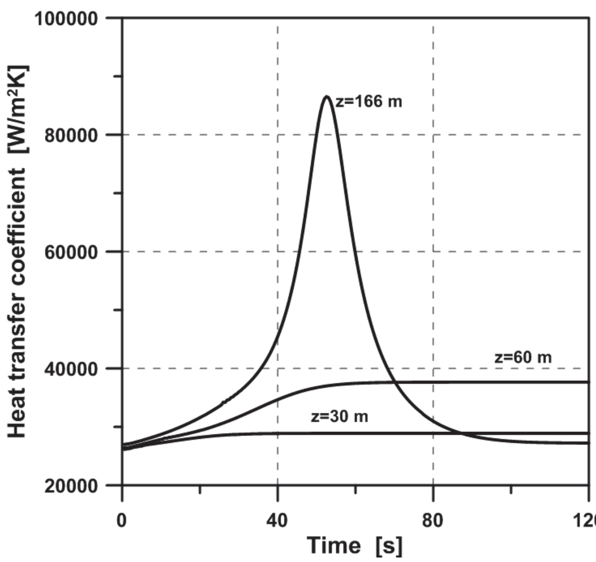

Fig. 9. Histories of the heat transfer coefficient in selected cross sections

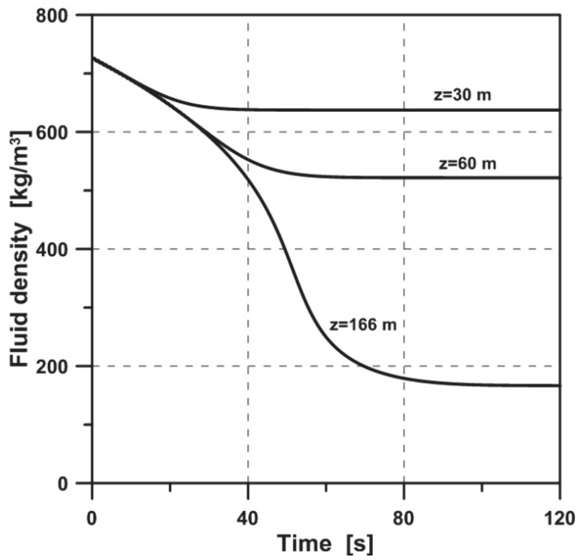

Fig. 10. Histories of the fluid density in selected cross sections

3.2. Experimental verification of the proposed method

The proposed model was verified experimentally by comparing calculated values of the fluid temperature in the supercritical boiler waterwall tubes to those obtained from measurements.

Based on the histories of measured values of pressure and the water mass flow in tubes (Fig. 11) as well as those of temperature (Fig. 12), the values of fluid temperature at the waterwall tube outlet were found and compared to the history of measured temperature values.

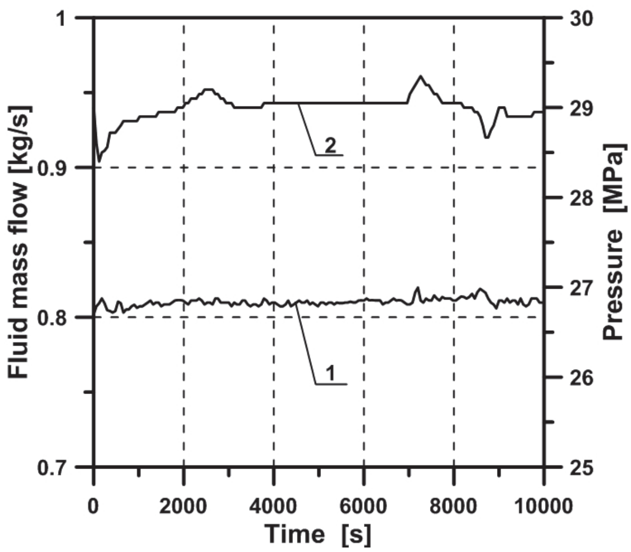

Fig. 11. Histories of measured values of the fluid mass flow in tubes (1) and of pressure (2)

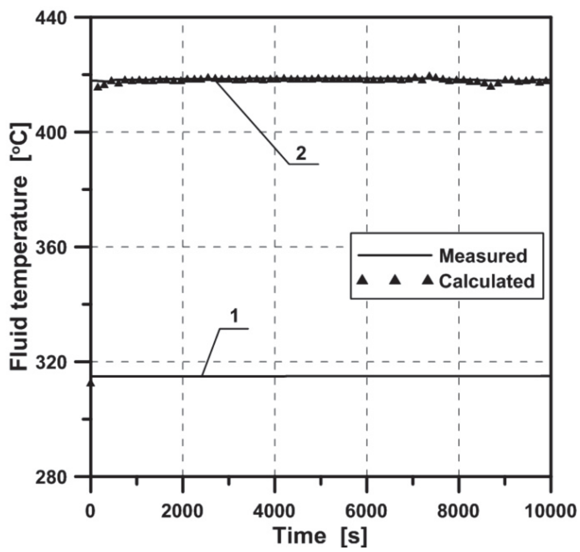

Fig. 12. Measured and calculated values of temperature: at the tube inlet (1); and at the tube outlet (2)

Fig. 11 and Fig. 12 present measurements and the results of calculations performed during the boiler steady-state operation. The curves in Fig. 11 illustrate changes in the pressure at the waterwall tubes inlet and the fluid mass flow history. In Fig. 12, the temperature values measured at the waterwall tube outlet are compared to the calculation results. Analysing the chart, a very good agreement can be seen between the results obtained from calculations and measurements.

The experimental verification of the proposed model fully proves its suitability for numerical modelling of thermal and flow phenomena in supercritical boiler waterwall tubes.

4. FINAL COMMENTS

In this paper, a mathematical model for the simulation of thermal and flow phenomena occurring on the side of the working fluid in the waterwalls of a supercritical boiler combustion chamber is proposed. It is a one-dimensional model with distributed parameters, based on the solution of equations describing the laws of mass, momentum, and energy conservation. Fluid density and temperature are determined on-line as the function of its enthalpy and pressure. All thermophysical properties of the fluid and waterwall pipe material are calculated in real time. The correctness of the determination of these properties in the on-line mode, especially for a fluid in the critical point area, is of great importance for the accuracy of obtained results. Also, the distribution of the heat transfer coefficient is determined on-line. In the proposed model, which has distributed parameters, computations are carried out in the direction of the working fluid flow in one tube. The tube is equal in size to those existing in a real facility. The fluid mass flow is also related to a single tube. The proposed method is based on the assumption that the operating fluid flows uniformly through all tubes of the combustion chamber waterwalls. The thermal load distribution along the combustion chamber height is known from the calculations of the heat exchange in the chamber, carried out with the zone method.

The developed methods were verified computationally. They were used for calculations with basic characteristic data, with regard to supercritical parameters for the combustion chamber of a boiler fired with brown coal. Results were compared to each other and a completely satisfactory convergence was achieved.

SYMBOLS

A	area, m^2
c	specific heat, J/(kg·K)
d	diameter, m
f	friction factor
g	thickness, m
G	mass flux, kg/(m^2·s)
h	enthalpy, kJ/kg
k	thermal conductivity coefficient, W/(m·K)
L	length, m
$\dot{m}$	mass flow, kg/s
M	number of cross-sections
n	number of tubes
p	pressure, Pa
p_τ	pressure drop by friction, Pa
$\dot{q}$	heat flux, W/m^2
$\dot{Q}$	heat transfer rate, W
r	radius, m
s	tube pitch, m
t	temperature, °C
U	circumference, m
w	velocity, m/s
z	space coordinate, m

Greek symbols

α	heat transfer coefficient, W/(m^2·K)
φ	tube inclination angle
μ	dynamic viscosity coefficient, Pa s
θ	wall temperature, °C
ρ	density, kg/m^3
σ	stress, MPa
τ	time, s, min
ψ	heat efficiency coefficient
ζ	friction factor
Δp	pressure drop, Pa
Δz	spatial size of control volume, m
$\Delta\tau$	time step, s

Subscripts

b	bulk
cg	combustion gases, combustion gas side
dht	deteriorated heat transfer
e	equivalent
f	fluid, fluid side
in	inner
inlet	inlet
j	subsequent control volume
m	mean
o	outer
out	outlet

t	total
w	wall

Non-dimensional numbers

Nu	Nusselt number (= $\alpha d_{in} / k$)
Pr	Prandtl number (= $\mu c / k$)
Re	Reynolds number (= $G d_{in} / \mu$)

REFERENCES

Adam E.J., Marchetti J.L., 1999. Dynamic simulation of large boilers with natural recirculation. *Comp. Chem. Eng.*, 23, 1031–1040. DOI: 10.1016/S0098-1354(99)00269-0.

Bird R.B., Stewart W.E., Lightfoot E.N., 2007. *Transport Phenomena*. 2nd edition, Wiley, New York.

Bishop A.A., Sandberg R.O., Tong L.S., 1965. Forced convection heat transfer to water at near-critical temperatures and supercritical pressures. *AIChE Chem. Eng. Symp. Ser.* 2, 77–85.

Błaszczuk A., Nowak W., Jagodzik Sz., 2014. Bed-to-wall heat transfer in a supercritical circulating fluidised bed boiler. *Chem. Process Eng.*, 35, 191-204. DOI:10.2478/cpe-2014-0015.

Fortran PowerStation 4.0, 1995. Microsoft Developer Studio. Microsoft Corporation.

Gerald C.F., Wheatley P.O., 1994. *Applied numerical analysis.* California Polytechnic State University, Addison-Wesley Publishing Company.

Grądziel S., 2012. *Modelling thermal and flow phenomena occurring in the evaporator of a boiler with natural circulation*. Publishing House of Cracow University of Technology, Cracow, Mechanika 406 (in Polish).

Grądziel S., 2008. Steam boiler furnace chamber calculations using the zone method, *Archiwum Energetyki*, XXXVIII (1), 191-202 (in Polish).

Jackson J.D., 2002. Consideration of the heat transfer properties of supercritical pressure water in connection with the cooling of advanced nuclear reactors. *Proc. of the 13th Pacific Basin Nuclear Conference*, Shenzhen City, China, 21-25 October 2002.

Kim H., Choi S., 2005. A model on water level dynamics in natural circulation drum-type boilers. *Int. Commun. Heat Mass Transfer International*, 32, 786–796. DOI: 10.1016/j.icheatmasstransfer.2004.10.010.

Kitoh K., Koshizuka S., Oka Yo., 1999. Refinement of transient criteria and safety analysis for a high temperature reactor cooled by supercritical water. *Proceedings of the 7th International Conference on Nuclear Engineering (ICONE-7)*, Tokyo, Japan, 19-23 April, Paper No. 7234.

Kotowicz J, Michalski S., 2014. Efficiency analysis of a hard-coal-fired supercritical power plant with a four-end high-temperature membrane for air separation. *Energy*, 64, 109-119. DOI: 10.1016/j.energy.2013.11.006.

Kuznetsov N.W., Nitor W.W., Dubovski I.E., Karasina E.S., 1973. *Thermal Calculations of Steam Boilers. Standard Method.* Energy, Moscow (in Russian).

Meyer C.A., 1993. *ASME Steam Tables: Thermodynamic and Transport Properties of Steam*. 6th edition, USA, New York : American Society of Mechanical Engineers 1993.

Modliński N., 2014. Computational modelling of a tangentially fired boiler with deposit formation phenomena. *Chem. Process Eng.*, 35, 361-398. DOI: 10.2478/cpe-2014-0027.

Pronobis S., Litka R., 2012. Rate of corrosion of waterwalls in supercritical pulverised fuel boilers. *Chem. Process Eng.*, 33, 263-277. DOI:10.2478/v10176-012-0026-x.

Slattery J.C., 1999. *Advanced Transport Phenomena.* Cambridge University Press, Cambridge.

Stosic Z., Stevanovic V., 2003. Numerical prediction of pipe CHF data with multi-fluid modelling approach. *Proceedings of the 11th International Conference on Nuclear Engineering – ICONE 11*, Tokyo, Japan, April 20–23, paper ICONE11-36382.

Taler D., Trojan M., Taler J., 2011, Mathematical modelling of tube heat exchangers with complex flow arrangement. *Chem. Process Eng.*, 32, 7-19. DOI: 10.2478/v10176-011-0001-y.

Taler J., Duda P., 2006. *Solving Direct and Inverse Heat Conduction Problems*. Springer-Verlag, Berlin.

Taler J. (Ed.), 2011. *Thermal and flow processes in large steam boilers. Modelling and monitoring*. PWN Warszawa (in Polish).

Taler J., 1981. Modelling temperature distribution in the boiler membrane walls. *Energetyka*, No 3 (in Polish).

Tang R., Yin F., Wang H., Chen T., 2007. An investigation into the heat transfer characteristics of spiral wall with internal rib in a supercritical sliding-pressure operation once-through boiler front. *Front. Energy Power Eng. China*, 1, 300–304. DOI: 10.1007/s11708-007-0043-5.

Tucakovic D.R., Stevanovic V.D., Zivanovic T., Jovovic A., Ivanović V.B., 2007. Thermal–hydraulic analysis of a steam boiler with rifled evaporating tubes. *Appl. Therm. Eng.* 27, 509–519. DOI: 10.1016/j.applthermaleng.2006.06.009.

Welty J.R., Wicks C.E., Wilson R.E., Rorrer G.L., 2008. *Fundamentals of momentum*, *heat and mass transfer*. 5th Ed., Wiley, Hoboken.

Water & Steam, 1999. IAPWS-IF97, Springer-Verlag.

Wojciechowski M., 2012. *Designing of the supercritical boilers on the example of steam boiler in Bełchatów Power Plant*. Final Project, Cracow University of Technology (in Polish).

Zima W., Grądziel S., 2013. *Simulation of transient processes in heating surfaces of power boilers*. LAMBERT Academic Publishing.

Zima W., Grądziel S., Cebula A., 2010. Modelling of heat and flow phenomena occurring in waterwall tubes of boilers for supercritical steam parameters. *Arch. Thermodyn.*, 31, 19-36. DOI: 10.2478/v10173-010-0012-y.

Received 11 March 2015
Received in revised form 16 December 2015
Accepted 20 December 2015